NASA Technical Memorandum 4321

Combined-Load Buckling Behavior of Metal-Matrix Composite Sandwich Panels Under Different Thermal Environments

William L. Ko and Raymond H. Jackson

SEPTEMBER 1991

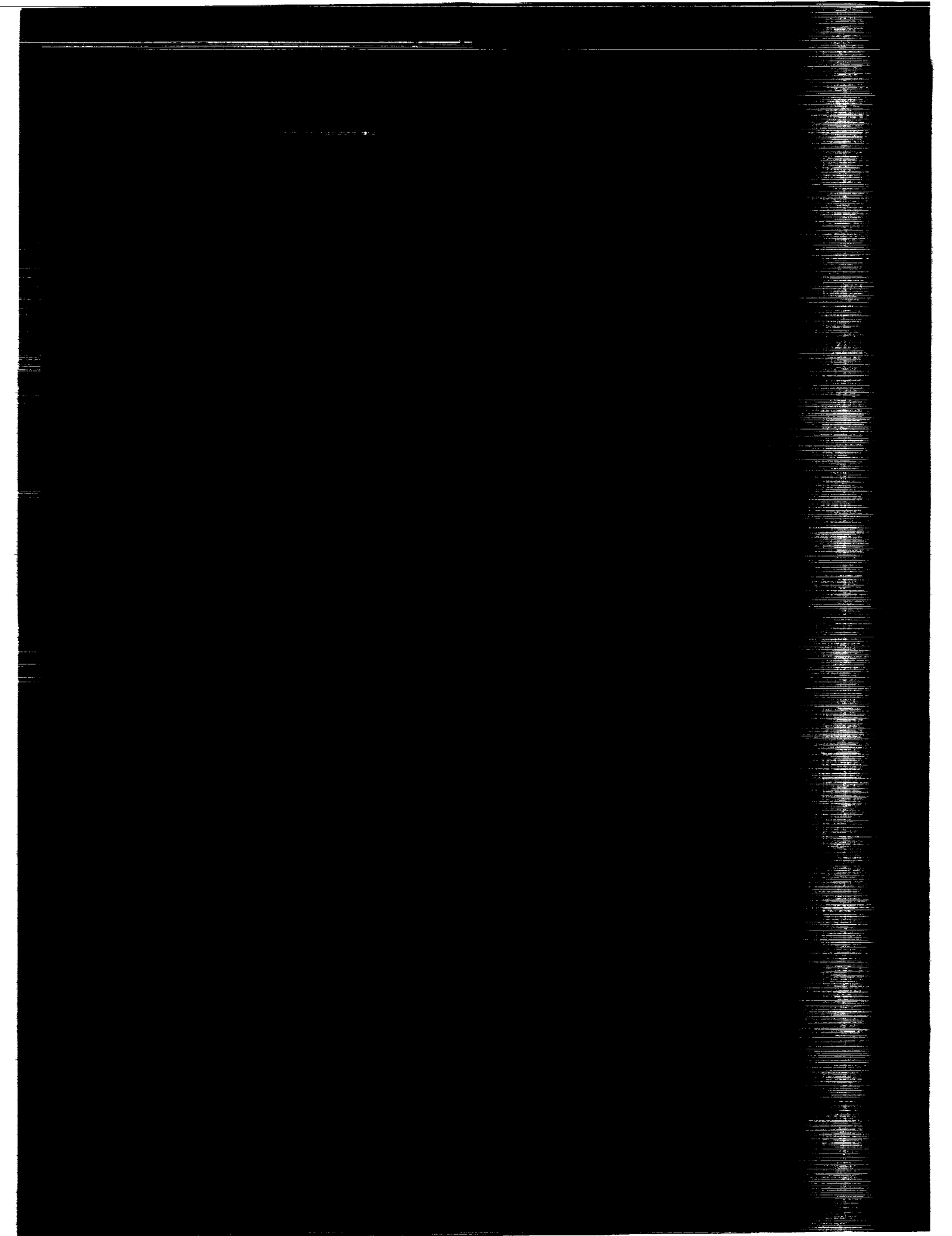

NASA Technical Memorandum 4321

Combined-Load Buckling Behavior of Metal-Matrix Composite Sandwich Panels Under Different Thermal Environments

William L. Ko and Raymond H. Jackson
Dryden Flight Research Facility
Edwards, California

National Aeronautics and
Space Administration
Office of Management
Scientific and Technical
Information Program
1991

CONTENTS

ABSTRACT

Combined compressive and shear buckling analysis was conducted on flat rectangular sandwich panels with the consideration of transverse shear effects of the core. The sandwich panel is fabricated with titanium honeycomb core and laminated metal-matrix composite face sheets. The results show that the square panel has the highest combined-load buckling strength, and that the buckling strength decreases sharply with the increases of both temperature and panel aspect ratio. The effect of layup (fiber orientation) on the buckling strength of the panels was investigated in detail. The metal-matrix composite sandwich panel was much more efficient than the sandwich panel with nonreinforced face sheets and had the same specific weight.

INTRODUCTION

Metal matrix composites (MMC) have gained considerable popularity as one of the strongest candidates for hot structural applications. Typical hot structures are the airframes of the hypersonic flight vehicles such as the national aero-space plane (NASP), gas turbine engine components, automobile engine components, etc. The MMC system is attractive to the hot structures because it can meet the structures' service requirements. Namely, MMC can operate at elevated temperatures and provide specific mechanical properties (i.e., high strength and high stiffness). Reference 1 discusses all the thermomechanical behavior of the MMC system.

The principal application of MMC in the hypersonic flight vehicles is in the form of sandwich constructions with the laminated MMC used as face sheets (ref. 2). The sandwich structure offers low thermal conductivity through the thickness, the high stiffness-to-weight ratio, and the capability to absorb thermal stresses.

During the service, the sandwich panel will be under the combined thermal and mechanical loading which could induce a critical situation of combined compressive and shear loading, the driving force of the panel buckling. Before actual application of MMC sandwich panels as hot structural components, the buckling characteristics of the structural panels under different thermal environments must be fully understood. This report investigates the combined compressive and shear buckling behavior of MMC sandwich panels and shows how the combined load buckling strength varies with temperature levels, fiber orientation, and panel geometry.

NOMENCLATURE

$A\ell$	aluminum
A_{mn}	Fourier coefficient of trial function for w, in.
a	length of sandwich panel, in.
a_{mn}^{ij}	coefficients of characteristic equations, no dimension
b	width of sandwich panel, in.
Cr	chromium
D^*	flexural stiffness parameter, $\frac{E_{Ti}I_s}{1-\nu_{Ti}^2}$, in-lb
D_{Qx}, D_{Qy}	transverse shear stiffnesses in planes parallel and normal to the corrugation axis (x-axis), lb/in
D_x, D_y	longitudinal and transverse panel flexural stiffnesses, E_xI_s, E_yI_s, in-lb
$\bar{D}_x, \bar{D}_y$	panel flexural stiffnesses, $D_x/(1-\nu_{xy}\nu_{yx})$, $D_y/(1-\nu_{xy}\nu_{yx})$, in-lb
D_{xy}	panel twisting stiffness, $2G_{xy}I_s$, in-lb

E_L, E_T	lamina Young's modulii, lb/in^2
E_{Ti}	Young's modulus of titanium material, lb/in^2
E_x, E_y	Young's modulii of face sheets, lb/in^2
G_{LT}	lamina shear modulus, lb/in^2
G_{cxz}, G_{cyz}	sheer modulii of sandwich core, lb/in^2
G_{xy}	shear modulus of face sheets, lb/in^2
h	depth of sandwich panel = distance between middle planes of two face sheets, in.
h_c	sandwich core depth, in.
I_s	moment of inertia, per unit width, of two face sheets taken with respect to horizontal centroidal axis (neutral axis) of the sandwich panel, $I_s = \frac{1}{2} t_s h^2 + \frac{1}{6} t_s{}^3$, in^4/in
i, j	index, 1,2,3, ...
k_x	compressive buckling load factor, $k_x = \frac{N_x a^2}{\pi^2 D^*}$, no dimension
k_{xy}	shear buckling load factor, $k_{xy} = \frac{N_{xy} a^2}{\pi^2 D^*}$, no dimension
MMC	metal matrix composites
m	number of buckle half waves in x-direction
NASP	national aero-space plane
N_x	normal stress resultants, lb/in
N_{xy}	shear stress resultant, lb/in
n	number of buckle half waves in y-direction
P	compressive load, lb
Q	shear load, lb
Q_x, Q_y	transverse shear force intensities, lb/in
SCS	silicon carbide fiber material
T	temperature, °F
t_s	thickness of sandwich face sheets, in.
V	vanadium
w	panel deflection, in.
x,y,z	rectangular Cartesian coordinates
$\delta_{mn\,ij}$	special delta function obeying $m \neq i$, $n \neq j$, $m \pm i = odd$, $n \pm j = odd$, $\delta_{mn\,ij} = \frac{mn\,ij}{(m^2 - i^2)(n^2 - j^2)}$
θ	fiber angle, deg
ν_{LT}	lamina Poisson ratio
ν_{Ti}	Poisson ratio of titanium material
ν_{xy}, ν_{yx}	Poisson ratios of face sheets, also for sandwich panel

METAL MATRIX COMPOSITE SANDWICH PANEL

Figure 1 shows a rectangular sandwich panel of length a and width b, fabricated with titanium honeycomb core of depth h_c and laminated metal matrix composite face sheets of same thickness t_s. The sandwich panel is subjected to combined compressive and shear loadings. The problem is to calculate buckling interaction curves for the panel, and to examine how the combined load buckling strength of the panel changes with (1) thermal environment, (2) fiber orientation, and (3) panel aspect ratio.

COMBINED-LOAD BUCKLING EQUATION

The combined-load (compression and shear) buckling characteristic equation developed by Ko and Jackson (ref. 3) for a simply supported anisotropic rectangular sandwich panel may be written as

$$\frac{M_{mn}}{k_{xy}} A_{mn} + \sum_{i=1}^{\infty} \sum_{j=1}^{\infty} \delta_{mnij} A_{ij} = 0 \tag{1}$$

This equation was derived through the use of the Rayleigh-Ritz method of minimization of the total potential energy of the sandwich panel with the effect of transverse shear taken into consideration.

In equation (1), A_{mn} is the undetermined Fourier coefficient of the assumed function for panel deflection w in the form

$$w(x,y) = \sum_{m=1}^{\infty} \sum_{n=1}^{\infty} A_{mn} \sin \frac{m\pi x}{a} \sin \frac{n\pi y}{b} \tag{2}$$

where a and b, respectively, are the length and the width of the panel and m and n, respectively, are the number of buckle half waves in the x- and y-directions. The δ_{mnij} in equation (1) is a special delta function defined as

$$\delta_{mnij} = \frac{mnij}{(m^2 - i^2)(n^2 - j^2)} \tag{3}$$

that obeys the conditions $m \neq i$, $n \neq j$, $m \pm i$ = odd, $n \pm j$ = odd. The stiffness factor M_{mn} in equation (1) is defined as

$$M_{mn} = \frac{ab}{32} \left\{ k_x \left(\frac{m\pi}{a} \right)^2 - \frac{a^2}{\pi^2 D^*} \left[a_{mn}^{11} + \underbrace{\frac{a_{mn}^{12}(a_{mn}^{23}a_{mn}^{31} - a_{mn}^{21}a_{mn}^{33}) + a_{mn}^{13}(a_{mn}^{21}a_{mn}^{32} - a_{mn}^{22}a_{mn}^{31})}{a_{mn}^{22}a_{mn}^{33} - a_{mn}^{23}a_{mn}^{32}}}_{\text{transverse sheer effect terms}} \right] \right\} \tag{4}$$

classical thin plate theory term

The compressive and shear buckling load factors k_x (eq. (4)) and k_{xy} (eq. (1)), respectively, are defined as

$$k_x = \frac{N_x a^2}{\pi^2 D^*} \quad \text{and} \quad k_{xy} = \frac{N_x a^2}{\pi^2 D^*} \tag{5}$$

where N_x and N_{xy}, respectively, are the panel compressive and shear buckling load intensities, and D^* is the flexural stiffness parameter, defined as

$$D^* = \frac{E_{Ti} I_s}{1 - \nu_{Ti}^2} \tag{6}$$

where $\{E_{Ti}\ \nu_{Ti}\}$ are the elastic constants associated with nonreinforced titanium material. The intensity of the moment of inertia I_s of the face sheets is taken with respect to the centroidal axis of the sandwich panel and is given by

$$I_s = \frac{1}{2}t_s h^2 + \frac{1}{6}t_s^3 \tag{7}$$

The characteristic coefficients a_{mn}^{ij} $(i, j = 1, 2, 3)$ appearing in equation (4) are defined as

$$a_{mn}^{11} = \bar{D}_x\left(\frac{m\pi}{a}\right)^4 + (\bar{D}_x\nu_{yx} + \bar{D}_y\nu_{xy} + 2D_{xy})\left(\frac{m\pi}{a}\right)^2\left(\frac{n\pi}{b}\right)^2 + \bar{D}_y\left(\frac{n\pi}{b}\right)^4 \tag{8}$$

$$a_{mn}^{12} = a_{mn}^{21} = -\left[\bar{D}_x\left(\frac{m\pi}{a}\right)^3 + \frac{1}{2}(\bar{D}_x\nu_{yx} + \bar{D}_y\nu_{xy} + 2D_{xy})\left(\frac{m\pi}{a}\right)\left(\frac{n\pi}{b}\right)^2\right] \tag{9}$$

$$a_{mn}^{13} = a_{mn}^{31} = -\left[\bar{D}_y\left(\frac{n\pi}{b}\right)^3 + \frac{1}{2}(\bar{D}_x\nu_{yx} + \bar{D}_y\nu_{xy} + 2D_{xy})\left(\frac{m\pi}{a}\right)^2\left(\frac{n\pi}{b}\right)\right] \tag{10}$$

$$a_{mn}^{22} = \bar{D}_x\left(\frac{m\pi}{a}\right)^2 + \frac{D_{xy}}{2}\left(\frac{n\pi}{b}\right)^2 + D_{Qx} \tag{11}$$

$$a_{mn}^{23} = a_{mn}^{32} = \frac{1}{2}(\bar{D}_x\nu_{yx} + \bar{D}_y\nu_{xy} + D_{xy})\left(\frac{m\pi}{a}\right)\left(\frac{n\pi}{b}\right) \tag{12}$$

$$a_{mn}^{33} = \bar{D}_y\left(\frac{n\pi}{b}\right)^2 + \frac{D_{xy}}{2}\left(\frac{m\pi}{a}\right)^2 + D_{Qy} \tag{13}$$

In equations (8) through (13), $\bar{D}_x$ and $\bar{D}_y$ are respectively defined as

$$\bar{D}_x = \frac{D_x}{1 - \nu_{xy}\nu_{yx}} \quad , \quad \bar{D}_y = \frac{D_y}{1 - \nu_{xy}\nu_{yx}} \tag{14}$$

and ν_{xy} and ν_{yx} are the panel Poisson ratios (also the Poisson ratios of the face sheets), D_x and D_y, respectively, are the axial and transverse flexural stiffnesses, D_{xy} is the twisting stiffness, and D_{Qx} and D_{Qy} are the transverse shear stiffnesses, given by

$$D_x = E_x I_s \quad , \quad D_y = E_y I_s \quad , \quad D_{xy} = 2G_{xy}I_s \quad , \quad D_{Qx} = G_{cxz}h_c \quad , \quad D_{Qy} = G_{cyz}h_c \tag{15}$$

EIGENVALUE SOLUTIONS

Equation (1) comprises a doubly infinite set of characteristic equations for all values of axial and transverse half-wave numbers m and n (i.e., mode shapes). However, the number of equations written from equation (1) may be truncated up to a certain finite number as required for convergency of eigenvalue solutions.

Because $m \pm i$ = odd and $n \pm j$ = odd (eq. (3)), then $(m \pm i) \pm (n \pm j) = (m \pm n) \pm (i \pm j)$ = even. Thus, if $m \pm n$ = even, then $(i \pm j)$ must be even also. Likewise, if $m \pm n$ = odd, then $(i \pm j)$ must also be odd. Therefore, there is no coupling between even case and odd case in each equation written out from equation (1) for a particular set of $\{m, n\}$. If the A_{mn} term in equation (1) is for $m \pm n$ = even, then the A_{ij} terms in the same equation must be for $(i \pm j)$ = even. Also, if the A_{mn} term is for $m \pm n$ = odd, then the A_{ij} terms must also be for $(i \pm j)$ = odd.

Thus, the set of simultaneous equations written out from equation (1) may be divided into two groups that are independent of each other; one group in which $m \pm n$ is even (symmetrical buckling), and the other group in

which $m \pm n$ is odd (antisymmetrical buckling) (refs. 3–7). For the deflection coefficients A_{mn} to have nontrivial solutions for given values of k_x and $\frac{b}{a}$, the determinant of the coefficients of the unknown A_{mn} must vanish. The largest eigenvalue $\frac{1}{k_{xy}}$ thus found will give the lowest buckling load factor k_{xy} as a function of k_x and $\frac{b}{a}$. Thus, a family of buckling interaction curves in the $k_x - k_{xy}$ space may be generated with $\frac{b}{a}$ as a parameter. Representative characteristic equations (buckling equations) for 12×12 matrices written out from equation (1) are shown in equations (16) and (17) for the cases $m \pm n =$ even and $m \pm n =$ odd (ref. 3).

For $m \pm n =$ even (symmetric buckling):

$$
\begin{array}{c|cccccccccccc|c}
 & A_{11} & A_{13} & A_{22} & A_{31} & A_{15} & A_{24} & A_{33} & A_{42} & A_{51} & A_{35} & A_{44} & A_{53} & \\
 & \frac{M_{11}}{k_{xy}} & 0 & \frac{4}{9} & 0 & 0 & \frac{8}{45} & 0 & \frac{8}{45} & 0 & 0 & \frac{16}{225} & 0 & \\
m=1,n=1 & & \frac{M_{13}}{k_{xy}} & -\frac{4}{5} & 0 & 0 & \frac{8}{7} & 0 & -\frac{8}{25} & 0 & 0 & \frac{16}{35} & 0 & \\
m=1,n=3 & & & \frac{M_{22}}{k_{xy}} & -\frac{4}{5} & -\frac{20}{63} & 0 & \frac{36}{25} & 0 & -\frac{20}{63} & \frac{4}{7} & 0 & \frac{4}{7} & \\
m=2,n=2 & & & & \frac{M_{31}}{k_{xy}} & 0 & -\frac{8}{25} & 0 & \frac{8}{7} & 0 & 0 & \frac{16}{35} & 0 & \\
m=3,n=1 & & & & & \frac{M_{15}}{k_{xy}} & -\frac{40}{27} & 0 & -\frac{8}{63} & 0 & 0 & -\frac{16}{27} & 0 & \\
m=1,n=5 & & & & & & \frac{M_{24}}{k_{xy}} & -\frac{72}{35} & 0 & -\frac{8}{63} & \frac{8}{3} & 0 & -\frac{120}{147} & \\
m=2,n=4 & & & \text{Symmetry} & & & & \frac{M_{33}}{k_{xy}} & -\frac{72}{35} & 0 & 0 & \frac{144}{49} & 0 & = 0 \\
m=3,n=3 & & & & & & & & \frac{M_{42}}{k_{xy}} & -\frac{40}{27} & -\frac{120}{147} & 0 & \frac{8}{3} & \\
m=4,n=2 & & & & & & & & & \frac{M_{51}}{k_{xy}} & 0 & -\frac{16}{27} & 0 & \\
m=5,n=1 & & & & & & & & & & \frac{M_{35}}{k_{xy}} & -\frac{80}{21} & 0 & \\
m=3,n=5 & & & & & & & & & & & \frac{M_{44}}{k_{xy}} & -\frac{80}{21} & \\
m=4,n=4 & & & & & & & & & & & & \frac{M_{53}}{k_{xy}} & \\
m=5,n=3 & & & & & & & & & & & & &
\end{array}
\tag{16}
$$

where the nonzero off-diagonal terms satisfy the conditions $m \neq i, n \neq j, m \pm i =$ odd, and $n \pm j =$ odd.

For $m \pm n$ = odd (antisymmetric buckling):

$$
\begin{array}{c|cccccccccccc|}
 & A_{12} & A_{21} & A_{14} & A_{23} & A_{32} & A_{41} & A_{16} & A_{25} & A_{34} & A_{43} & A_{52} & A_{61} \\
 & \frac{M_{12}}{k_{xy}} & -\frac{4}{9} & 0 & \frac{4}{5} & 0 & -\frac{8}{45} & 0 & \frac{20}{63} & 0 & \frac{8}{25} & 0 & -\frac{4}{35} \\
m=1,n=2 & & \frac{M_{21}}{k_{xy}} & -\frac{8}{45} & 0 & \frac{4}{5} & 0 & -\frac{4}{35} & 0 & \frac{8}{25} & 0 & \frac{20}{63} & 0 \\
m=2,n=1 & & & \frac{M_{14}}{k_{xy}} & -\frac{8}{7} & 0 & -\frac{16}{225} & 0 & \frac{40}{27} & 0 & -\frac{16}{35} & 0 & -\frac{8}{175} \\
m=1,n=4 & & & & \frac{M_{23}}{k_{xy}} & -\frac{36}{25} & 0 & -\frac{4}{9} & 0 & \frac{72}{35} & 0 & -\frac{4}{7} & 0 \\
m=2,n=3 & & & & & \frac{M_{32}}{k_{xy}} & -\frac{8}{7} & 0 & -\frac{4}{7} & 0 & \frac{72}{35} & 0 & -\frac{4}{9} \\
m=3,n=2 & & & & & & \frac{M_{41}}{k_{xy}} & -\frac{8}{175} & 0 & -\frac{16}{35} & 0 & \frac{40}{27} & 0 \\
m=4,n=1 & & & & & & & \frac{M_{16}}{k_{xy}} & -\frac{20}{11} & 0 & -\frac{8}{45} & 0 & -\frac{36}{1225} \\
m=1,n=6 & & & \text{Symmetry} & & & & & \frac{M_{25}}{k_{xy}} & -\frac{8}{3} & 0 & -\frac{100}{441} & 0 \\
m=2,n=5 & & & & & & & & & \frac{M_{34}}{k_{xy}} & -\frac{144}{49} & 0 & -\frac{8}{45} \\
m=3,n=4 & & & & & & & & & & \frac{M_{43}}{k_{xy}} & -\frac{8}{3} & 0 \\
m=4,n=3 & & & & & & & & & & & \frac{M_{52}}{k_{xy}} & -\frac{20}{11} \\
m=5,n=2 & & & & & & & & & & & & \frac{M_{61}}{k_{xy}} \\
m=6,n=1 & & & & & & & & & & & &
\end{array}
= 0 \qquad (17)
$$

where the nonzero off-diagonal terms satisfy the conditions $m \neq i$, $n \neq j$, $m \pm i$ = odd, and $n \pm j$ = odd.

Notice that the diagonal terms in equations (16) and (17) came from the first term of equation (1), and the series term of equation (1) gives the off-diagonal terms of the matrices. The 12 × 12 determinant was found to give sufficiently accurate eigenvalue solutions.

NUMERICAL RESULTS

Physical Properties of Panels

The sandwich panels analyzed have the following geometry:

$$a = 24 \text{ in.}$$
$$\frac{b}{a} = 1, 2, 3, 4$$
$$h = 1.2 \text{ in.}$$
$$h_c = h - t_s = 1.1680 \text{ in.}$$
$$t_s = 0.0320 \text{ in.}$$

The effective material properties used for titanium honeycomb core are shown in table 1.

Table 1. Material properties of titanium honeycomb.

Temperature, °F	G_{cxz}, 10^5 lb/in^2	G_{cyz}, 10^5 lb/in^2
70	2.0835	0.9435
600	1.8100	0.8197
1200	1.2005	0.6566

Unpublished material properties (provided by the McDonnell Douglas Corporation, St. Louis, Missouri) of the Sic fiber/$Ti-15V-3Cr-35n-3A\ell$ metal matrix ($SCS-6/Ti-15-3$) composite lamina are listed in table 2.

Table 2. Material properties of $SCS-6/Ti-15-3$ metal matrix composite lamina.

Temperature, °F	E_L, 10^6 lb/in^2	E_T, 10^6 lb/in^2	G_{LT}, 10^6 lb/in^2	ν_{LT}
70	27.72	18.09	8.15	0.3
600	25.30	13.70	5.90	0.3
1200	23.22	8.69	3.50	0.3
1800	22.59	2.70	1.04	0.3

Table 3 lists material properties that were derived from the lamina data of table 2 using lamination theory for two different laminates.

Table 3. Material properties of $SCS-6/Ti-15-3$ laminated metal-matrix composites.

Temperature, °F	$E_x \times 10^6$ lb/in^2	$E_y \times 10^6$ lb/in^2	$G_{xy} \times 10^6$ lb/in^2	$\nu_{xy} = \nu_{yx}$
	[90 / 0 / 0 / 90] laminate			
70	22.9679	22.9679	8.150	0.2369
600	19.5884	19.5884	5.900	0.2108
1200	16.0703	16.0703	3.500	0.1634
1800	12.7301	12.7301	1.040	0.0641
	[45 / −45 / −45 / 45] laminate			
70	21.1545	21.1545	9.2843	0.2972
600	15.9953	15.9953	8.0892	0.3555
1200	10.2608	10.2608	6.9066	0.4658
1800	3.6082	3.6082	5.9819	0.7347

Finally, for the value of D^* (eq. (6)), the room temperature material properties of $Ti-6-4$ were used. Namely, $E_{Ti} = 16 \times 10^6$ lb/in^2, $\nu_{Ti} = 0.31$.

Buckling Curves

Figure 2 shows a family of buckling interaction curves calculated from equation (1) for the sandwich panels with two different types of laminated face sheets. The buckling interaction curves are plotted for different panel aspect ratios $\frac{b}{a}$ and different temperatures using data given in table 3. For $\frac{b}{a} = 1$ (square panel), all of the buckling interaction

curves are continuous and are associated with symmetric buckling. The antisymmetric buckling interaction curves for $\frac{b}{a} = 1$ (not shown) give much higher buckling loads. For $\frac{b}{a} = 2, 3, 4$, the buckling interaction curves are discontinuous, and are the composite curves consisting of both symmetric and antisymmetric buckling interaction curve segments. For $\frac{b}{a} = 1$, the [45 / −45 / −45 / 45] lamination case has higher combined buckling strength as compared with the [90 / 0 / 0 / 90] lamination case. As the temperature increases, the buckling strength of the latter decreases slightly faster than the former. For $\frac{b}{a} = 2$, the two lamination cases have comparable compression-dominated buckling strength. But for shear-dominated buckling, the [45 / −45 / −45 / 45] lamination case is slightly superior to the [90 / 0 / 0 / 90] lamination case. For $\frac{b}{a} = 3, 4$, the [90 / 0 / 0 / 90] lamination case has slightly higher compression-dominated buckling strength than the [45 / −45 / −45 / 45] lamination. For shear-dominated loadings, both cases have very close buckling strengths. Even though the [45 / −45 / −45 / 45] lamination case has lower values of bending stiffness $\{D_x, D_y\}$ (or $\{E_x, E_y\}$, table 3) than the [90 / 0 / 0 / 90] lamination case, it has higher twisting D_{xy} (or G_{xy}, table 3) than the latter for all the temperature levels. Because the combined-load buckling strength of panels depend not only on $\{D_x, D_y\}$ but also on D_{xy} (eqs. (1), (4), and (8) through (13)), the combination of the values of D_x, D_y, and D_{xy} happened to cause the [45 / −45 / −45 / 45] lamination case to have higher buckling resistance than the [90 / 0 / 0 / 90] lamination case.

Figure 3 shows the room temperature (T = 70°F) buckling interaction curves for the square ($\frac{b}{a} = 1$) sandwich panels with [90 / 0 / 0 / 90] and [45 / −45 / −45 / 45] laminated face sheets (taken from fig. 2) compared with similar sandwich panels fabricated with nonreinforced titanium face sheets and having the same specific weight as the other two types of sandwich panels (ref. 3). Notice that through the fiber reinforcement of the face sheets, the buckling strength of the sandwich panel could be boosted by 32 percent in pure compression and by 26 percent in pure shear.

Figures 4 and 5, respectively, show the decreases of the compressive and shear buckling strengths (k_x, k_{xy}) of the two types of metal matrix composite sandwich panels with the increase of the panel aspect ratio $\frac{b}{a}$. The compressive strength (k_x) decreases sharply by approximately 50 percent when $\frac{b}{a}$ increases from 1 to 2 (fig. 4). Beyond $\frac{b}{a} = 2$, the decrease of k_x gradually dies out. But the shear buckling strength (k_{xy}) (fig. 5) is less sensitive to the change of $\frac{b}{a}$. Figure 6 shows the degradation of k_x of pure compression, and k_{xy} of pure shear with the increase in temperature for the square panel. The [45 / −45 / −45 / 45] lamination case has a lower rate of degradation of k_x and k_{xy} with temperature than the [90 / 0 / 0 / 90] lamination case. Table 4 lists the buckling data for the sandwich panels studied.

Table 4. Buckling load factors for pure compression and pure shear at different temperatures and aspect ratios.*

Layup	$\frac{b}{a}$	Temperature, °F	k_x	k_{xy}, even	k_{xy}, odd
[90 / 0 / 0 / 90]	1	70	3.93242	7.71718	9.34069
		600	3.18011	6.32870	7.75663
		1200	2.35383	4.70545	5.85583
	1.2	70	2.90790	7.01805	8.24045
		600	2.35359	5.75184	6.81654
		1200	1.74584	4.27731	5.13322
	1.4	70	2.38263	6.70870	7.41718
		600	1.93504	5.50804	6.11211
		1200	1.44494	4.11233	4.58331
	1.6	70	2.08085	6.58142	6.83571
		600	1.69709	5.41644	5.61720
		1200	1.27741	4.06344	4.19768

Table 4. Continued.

Layup	$\frac{b}{a}$	Temperature, $^{\circ}F$	k_x	k_{xy}, even	k_{xy}, odd
[90 / 0 / 0 / 90]	1.8	70	1.89232	6.51732	6.44253
		600	1.54976	5.37342	5.28587
		1200	1.17558	4.04519	3.94307
	2	70	1.76679	6.44160	6.18724
		600	1.45244	5.13322	5.07409
		1200	1.10938	4.00212	3.78455
	3	70	1.50153	5.82618	5.86396
		600	1.24936	4.78149	4.82515
		1200	0.97520	3.57359	3.62592
	4	70	1.41951	5.74023	5.75026
		600	1.18758	4.72080	4.72285
		1200	0.93590	3.54733	3.53852
[45 / −45 / −45 / 45]	1	70	4.03816	7.85897	9.38815
		600	3.38572	6.60935	7.84719
		1200	2.67307	5.13964	5.99516
	1.2	70	2.97685	7.12846	8.29900
		600	2.48778	5.97041	6.92963
		1200	1.95522	4.62051	5.30484
	1.4	70	2.42410	6.78287	7.49014
		600	2.01563	5.65453	6.25421
		1200	1.57146	4.34675	4.80101
	1.6	70	2.10210	6.62335	6.91567
		600	1.73829	5.49873	5.77352
		1200	1.34290	4.19962	4.43965
	1.8	70	1.89858	6.53808	6.52153
		600	1.56176	5.41298	5.44047
		1200	1.19577	4.11457	4.18453
	2	70	1.76180	6.45794	6.25967
		600	1.44240	5.34228	5.21534
		1200	1.09538	4.05281	4.00707
	3	70	1.46765	5.87695	5.88705
		600	1.18320	4.87905	4.86843
		1200	0.87404	3.72769	3.69934
	4	70	1.37481	5.76033	5.78450
		600	1.10042	4.75863	4.78720
		1200	0.82212	3.61300	3.64039

*Sandwich panels with $SCS-6/Ti-15-3$ metal matrix composite face sheets and $Ti-6-4$ honeycomb core.

Effect of Fiber Orientations

Figure 7 shows the room temperature (T = 70°F) pure compression buckling strength (k_x) of sandwich panel with $[\theta/-\theta/-\theta/\theta]$ laminated face sheets plotted as a function of fiber angle θ with panel aspect ratio $\frac{b}{a}$ as a parameter. The square ($\frac{b}{a}$ = 1) sandwich panel with [45 / −45 / −45 / 45] laminated face sheets shows the highest compressive

buckling strength (maximum k_x). This special feature of composite material was also seen in single laminated plates with symmetric angle-ply laminate (ref. 7) and antisymmetric angle-ply laminate (ref. 8). Similar plots for pure-shear buckling strength (k_{xy}) are shown in figure 8. For $\frac{b}{a} = 1$, the maximum k_{xy} occurs at approximately $\theta = 30°$. As the panel aspect ratio increases, the maximum k_{xy} point migrates within the region $0 \leq \theta \leq 30°$. Table 5 shows the data for plotting figures 7 and 8.

Table 5. Buckling load factors for pure compression and pure shear for different face sheet fiber orientations.*

Layup	$\frac{b}{a}$	k_x	k_{xy}, even	k_{xy}, odd
[0 / 0 / 0 / 0]	1	3.96003	7.81468	9.32944
	1.2	3.05113	7.28798	8.23109
	1.4	2.57877	7.08318	7.46504
	1.6	2.30387	6.99602	6.96156
	1.8	2.13018	6.90756	6.64697
	2	2.01344	6.76707	6.46216
	3	1.76237	6.15904	6.26618
	4	1.68308	6.25476	6.13859
[15 / −15 / −15 / 15]	1	3.98355	7.84286	9.36001
	1.2	3.04971	7.28497	8.26229
	1.4	2.56328	7.05871	7.48940
	1.6	2.27968	6.96204	6.97494
	1.8	2.10024	6.87744	6.64806
	2	1.97949	6.74842	6.45136
	3	1.71931	6.13628	6.23358
	4	1.63696	6.19784	6.10674
[30 / −30 / −30 / 30]	1	4.02685	7.88368	9.40620
	1.2	3.03207	7.24682	8.31079
	1.4	2.51245	6.96575	7.52089
	1.6	2.20888	6.84180	6.97885
	1.8	2.01650	6.76092	6.62110
	2	1.88689	6.65770	6.39444
	3	1.60710	6.04856	6.11200
	4	1.51836	6.02579	5.99300
[45 / −45 / −45 / 45]	1	4.03816	7.85897	9.38815
	1.2	2.97685	7.12846	8.29900
	1.4	2.42410	6.78287	7.49014
	1.6	2.10210	6.62335	6.91567
	1.8	1.89858	6.53808	6.52153
	2	1.76180	6.45794	6.25967
	3	1.46765	5.87695	5.88705
	4	1.37481	5.76033	5.78450
[60 / −60 / −60 / 60]	1	3.99183	7.74021	9.27789
	1.2	2.88404	6.93235	8.20249
	1.4	2.31251	6.53572	7.38059
	1.6	1.98247	6.34780	6.77936
	1.8	1.77544	6.25607	6.35471

Table 5. Concluded.

Layup	$\frac{b}{a}$	k_x	k_{xy}, even	k_{xy}, odd
[60 / −60 / −60 / 60]	2	1.63718	6.19029	6.06348
	3	1.34323	5.65217	5.61073
	4	1.25172	5.46461	5.52447
[75 / −75 / −75 / 75]	1	3.92383	7.59910	9.14721
	1.2	2.79409	6.74426	8.08839
	1.4	2.21764	6.31953	7.26086
	1.6	1.88814	6.11773	6.64295
	1.8	1.68331	6.02428	6.19889
	2	1.54757	5.96786	5.88939
	3	1.26294	5.46423	5.38919
	4	1.17586	5.23727	5.31436
[90 / −90 / −90 / 90]	1	3.89159	7.53591	9.08904
	1.2	2.75642	6.66586	8.03805
	1.4	2.18004	6.23284	7.20937
	1.6	1.85211	6.02771	6.58591
	1.8	1.64910	5.93475	6.13524
	2	1.51505	5.88213	5.81963
	3	1.23578	5.39127	5.30489
	4	1.15106	5.15211	5.23445

* Sandwich panels with $SCS-6/Ti-15-3$ metal matrix composite face sheets and $Ti-6-4$ honeycomb core.

CONCLUSIONS

Combined compressive and shear buckling analysis was performed on flat rectangular sandwich panels fabricated with titanium honeycomb core and laminated metal matrix composite face sheets.

The square panel has the highest combined-load buckling strength, and the buckling strength decreases sharply with the increases of both temperature and panel aspect ratio. The [45 / −45 / −45 / 45] lamination case had higher combined-load buckling strength than the [90 / 0 / 0 / 90] lamination case for panel aspect ratio 1. For panel aspect ratio 2, the two lamination cases have comparable compression-dominated buckling strength. But the [45 / −45 / −45 / 45] lamination case has slightly superior buckling strength as compared with the [90 / 0 / 0 / 90] lamination case in the shear-dominated loading. For $\frac{b}{a} = 3, 4$, the [90 / 0 / 0 / 90] lamination case has slightly higher compression-dominated buckling strength than the [45 / −45 / −45 / 45] lamination. For shear-dominated loadings, both cases have very close buckling strengths.

The geometry of a metallic matrix sandwich panel for the optimum compressive buckling strength is square and has [45 / −45 / −45 / 45] lamination. For optimum shear buckling strength, the panel is square and has [30 / −30 /−30 / 30] lamination.

The combined load buckling strength of the sandwich panel could be raised considerably through fiber reinforcement of face sheets.

Dryden Flight Research Facility
National Aeronautics and Space Administration
Edwards, California, April 15, 1991

REFERENCES

1. Taya, Minoru and Richard J. Arsenault, *Metal Matrix Composites: Thermomechanical Behavior*, Pergamon Press, NY, 1989.

2. Tenny, Darrel R., W. Barry Lisagor, and Sidney C. Dixon, "Materials and Structures for Hypersonic Vehicles," *J. Aircraft*, vol. 26, no. 11, Nov. 1989, pp. 953–970.

3. Ko, William L. and Raymond H. Jackson, *Combined Compressive and Shear Buckling Analysis of Hypersonic Aircraft Structural Sandwich Panels*, NASA TM - 4290, 1991.

4. Bert, Charles W. and K.N. Cho, "Uniaxial Compressive and Shear Buckling in Orthotropic Sandwich Plates By Improved Theory," AIAA 86–0977, May 1986.

5. Batdorf, S.B. and Manuel Stein, *Critical Combinations of Shear and Direct Stress for Simply Supported Rectangular Flat Plates*, NACA TN-1223, 1947.

6. Stein, Manuel and John Neff, *Buckling Stresses of Simply Supported Rectangular Flat Plates in Shear*, NACA TN-1222, 1947.

7. Aston, J.E. and J.M. Whitney, *Theory of Laminated Plates*, Technomic Publishing Co., Westport, CT, 1970.

8. Jones, Robert M., Harold S. Morgan, and James M. Whitney, "Buckling and Vibration of Antisymmetrically Laminated Angle-Ply Rectangular Plates," *J. Appl. Mech.*, vol. 40, no. 4, Dec. 1973, pp. 1143–1144.

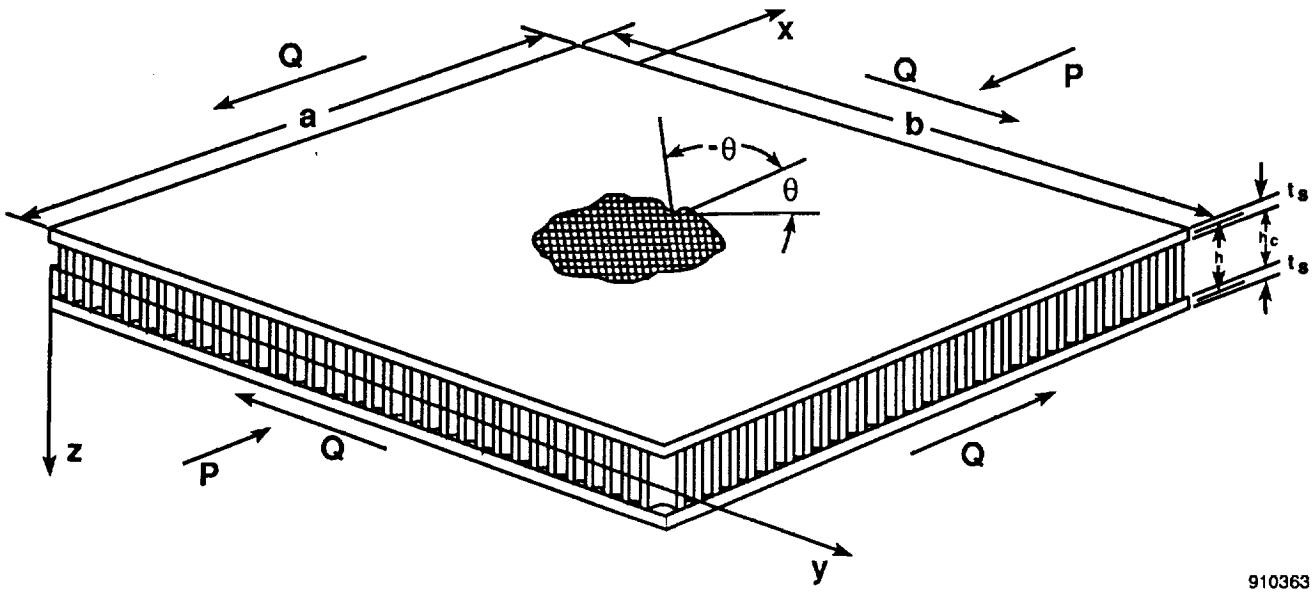

Figure 1. Honeycomb core sandwich panel with metal matrix composite face sheets subjected to combined compressive and shear loadings.

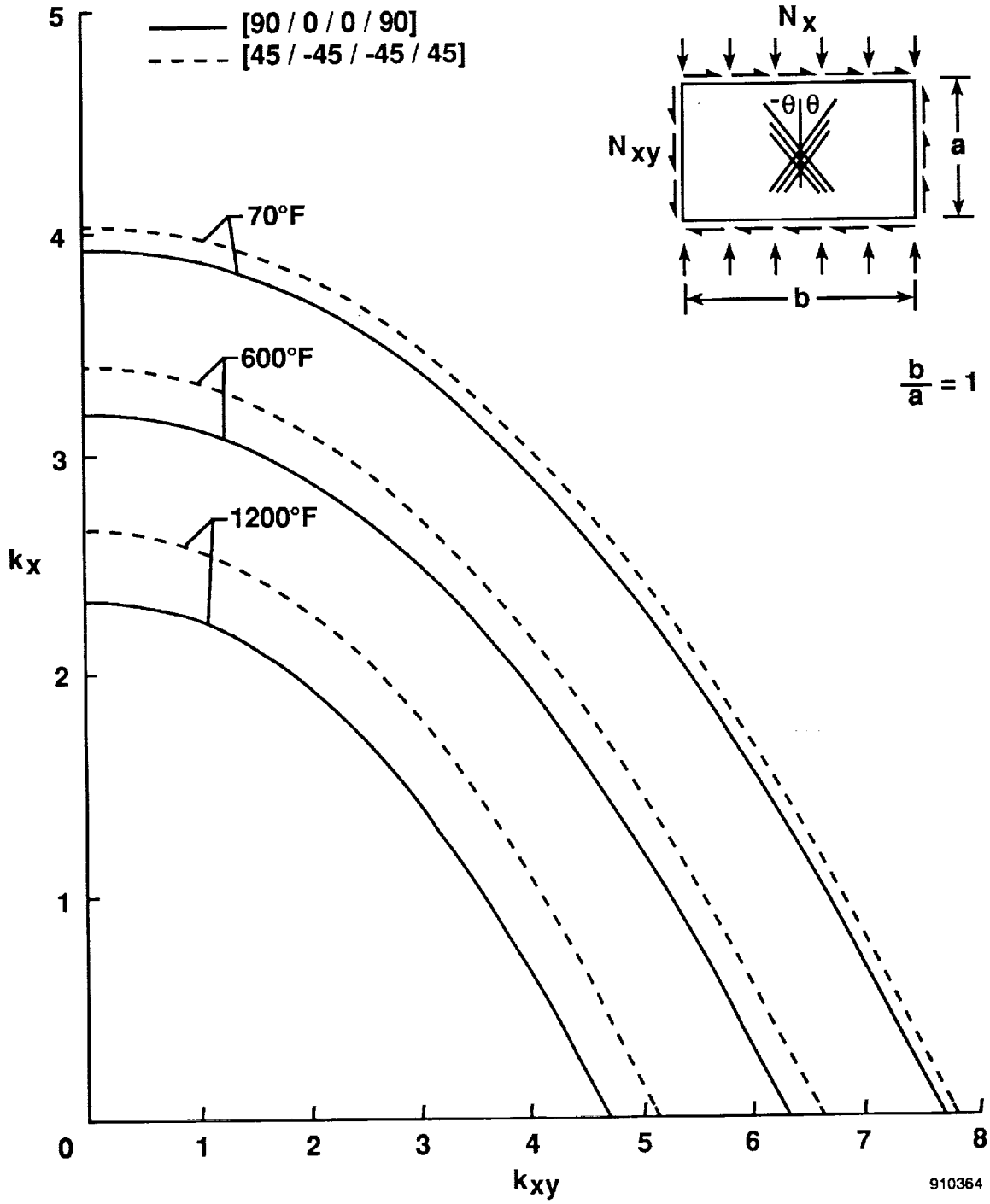

Figure 2. Buckling interaction curves for metal matrix composite sandwich panels at different temperatures. All curves symmetrical buckling; $SCS - 6/Ti - 15 - 3$ composite face sheets; $Ti - 6 - 4$ honeycomb core.

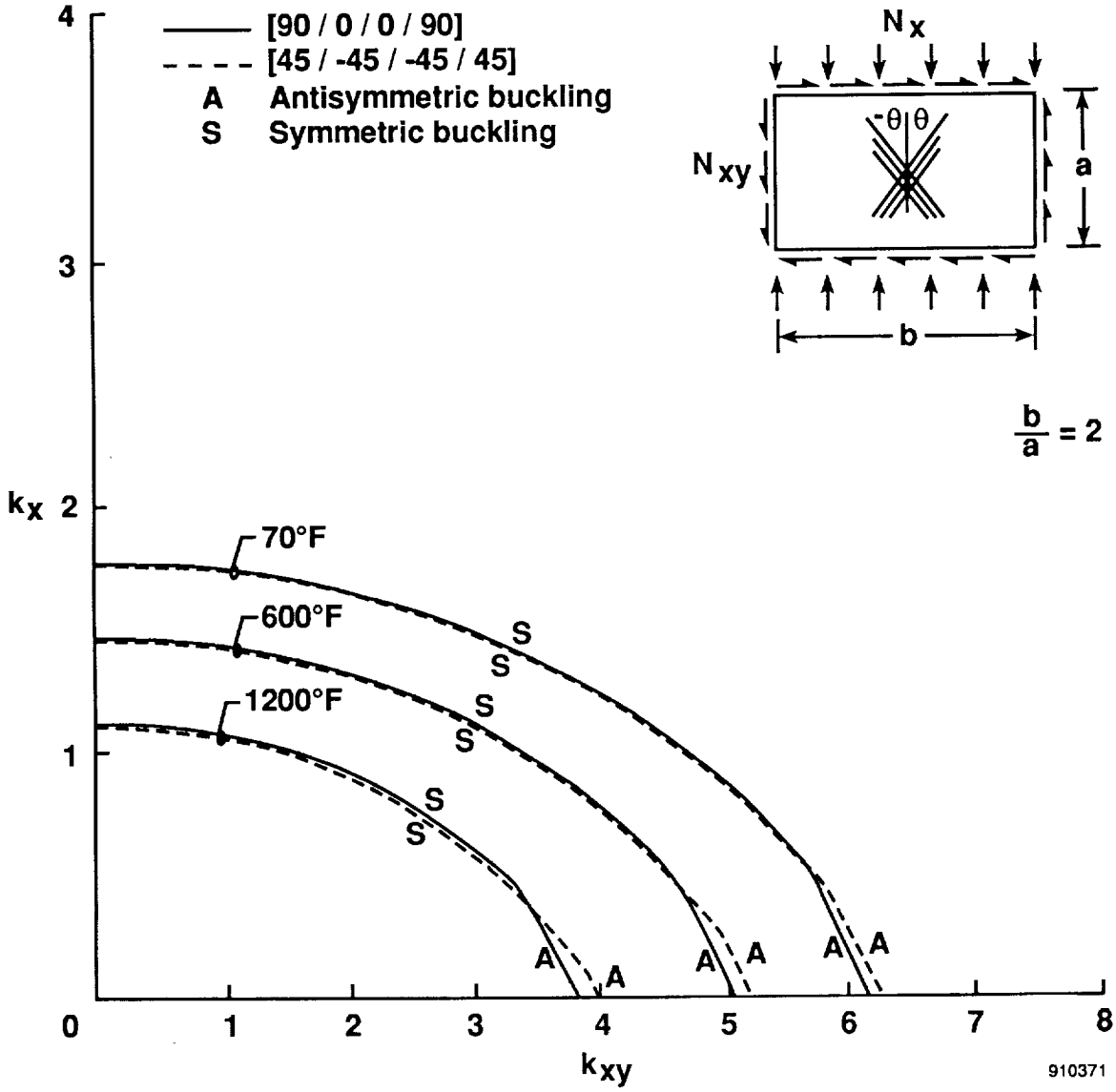

Figure 2. Continued.

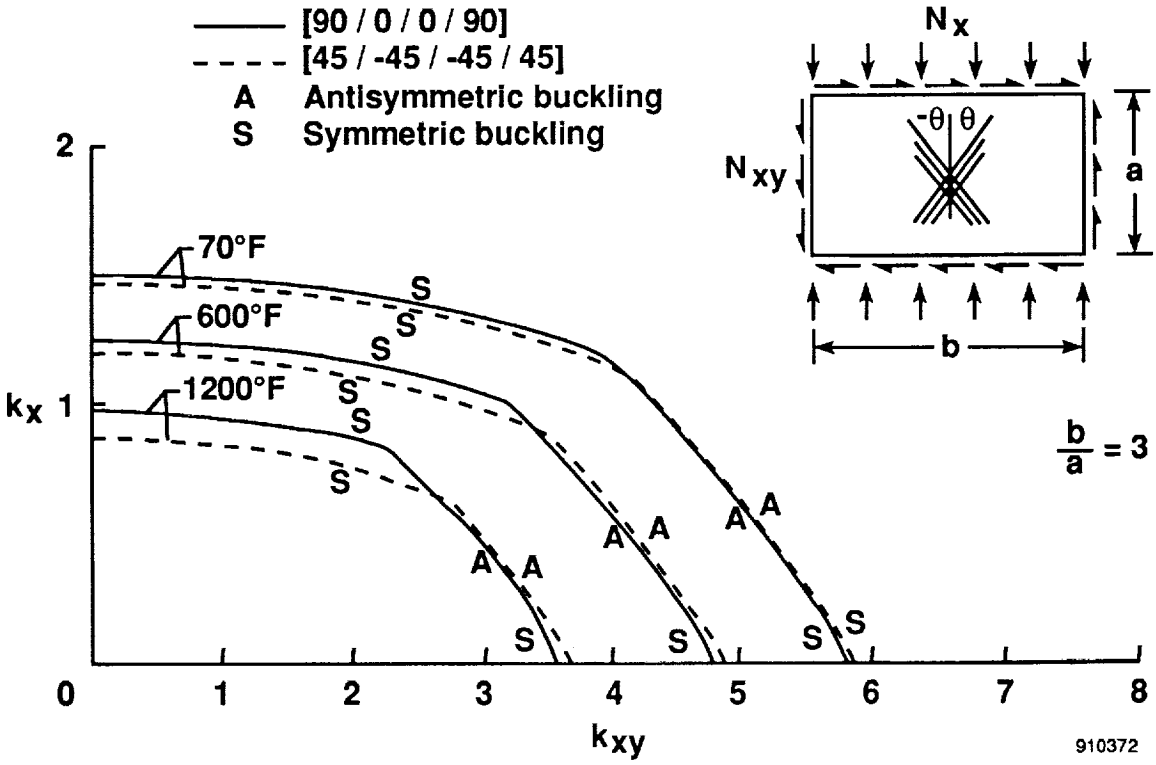

Figure 2. Continued.

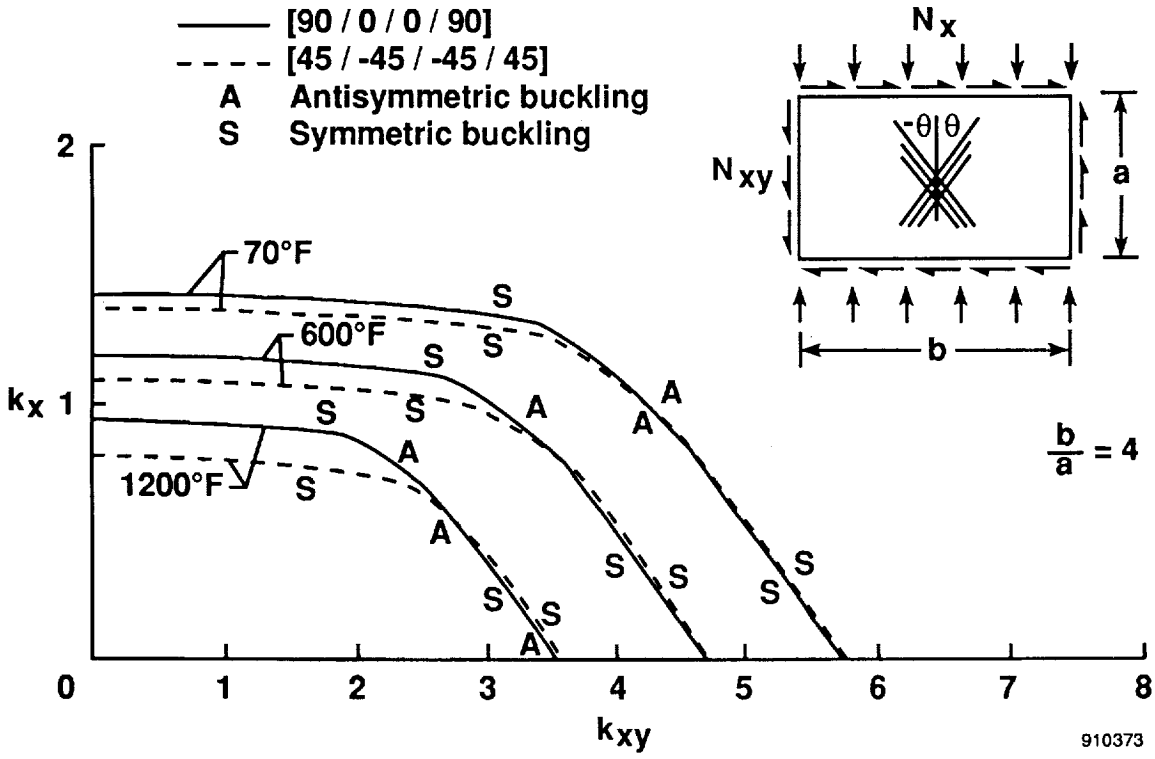

Figure 2. Concluded.

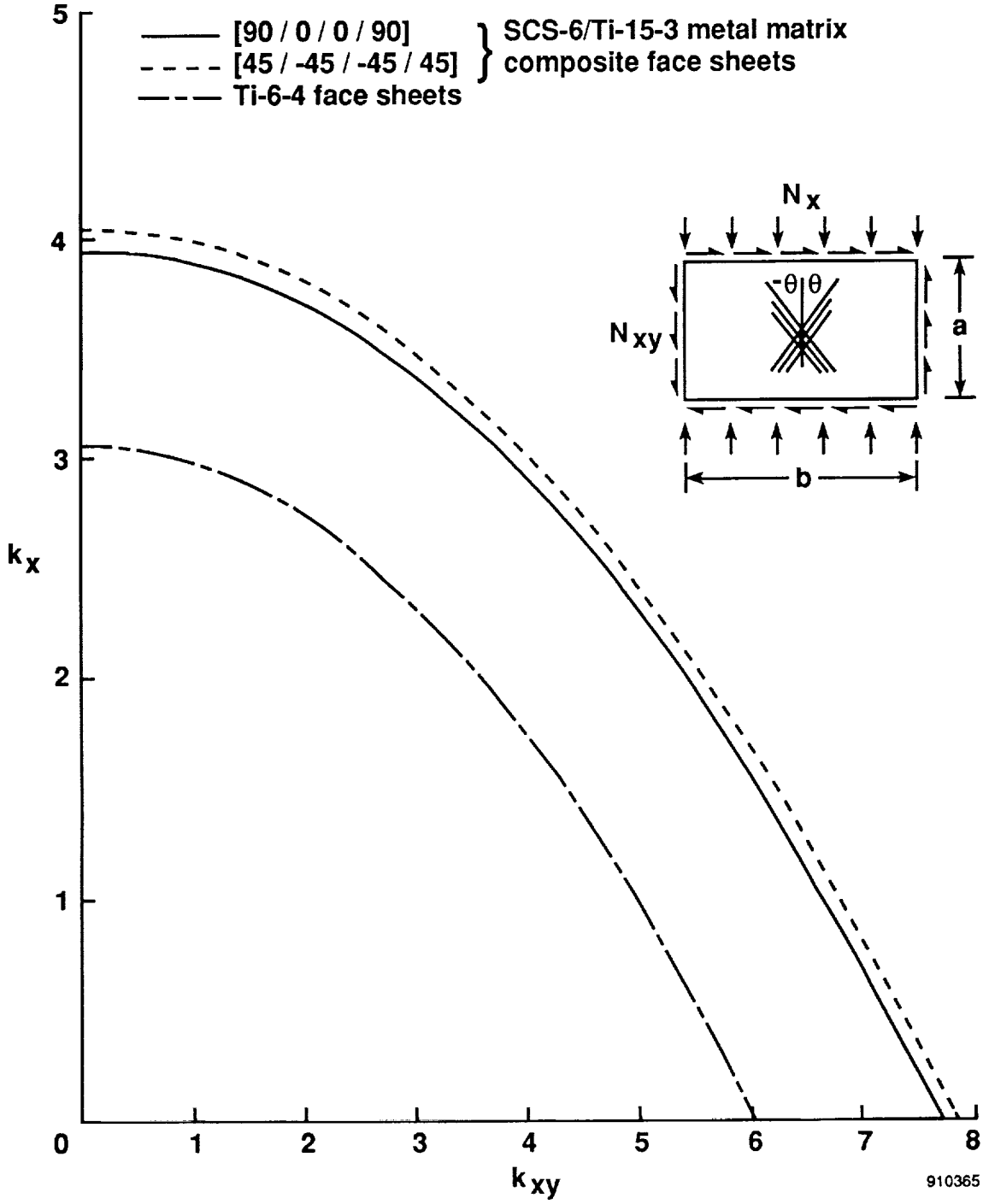

Figure 3. Comparison of buckling strengths of honeycomb-core sandwich panels of same specific weight fabricated with different face sheet materials; $b/a = 1, T = 70°F; Ti - 6 - 4$ honeycomb core.

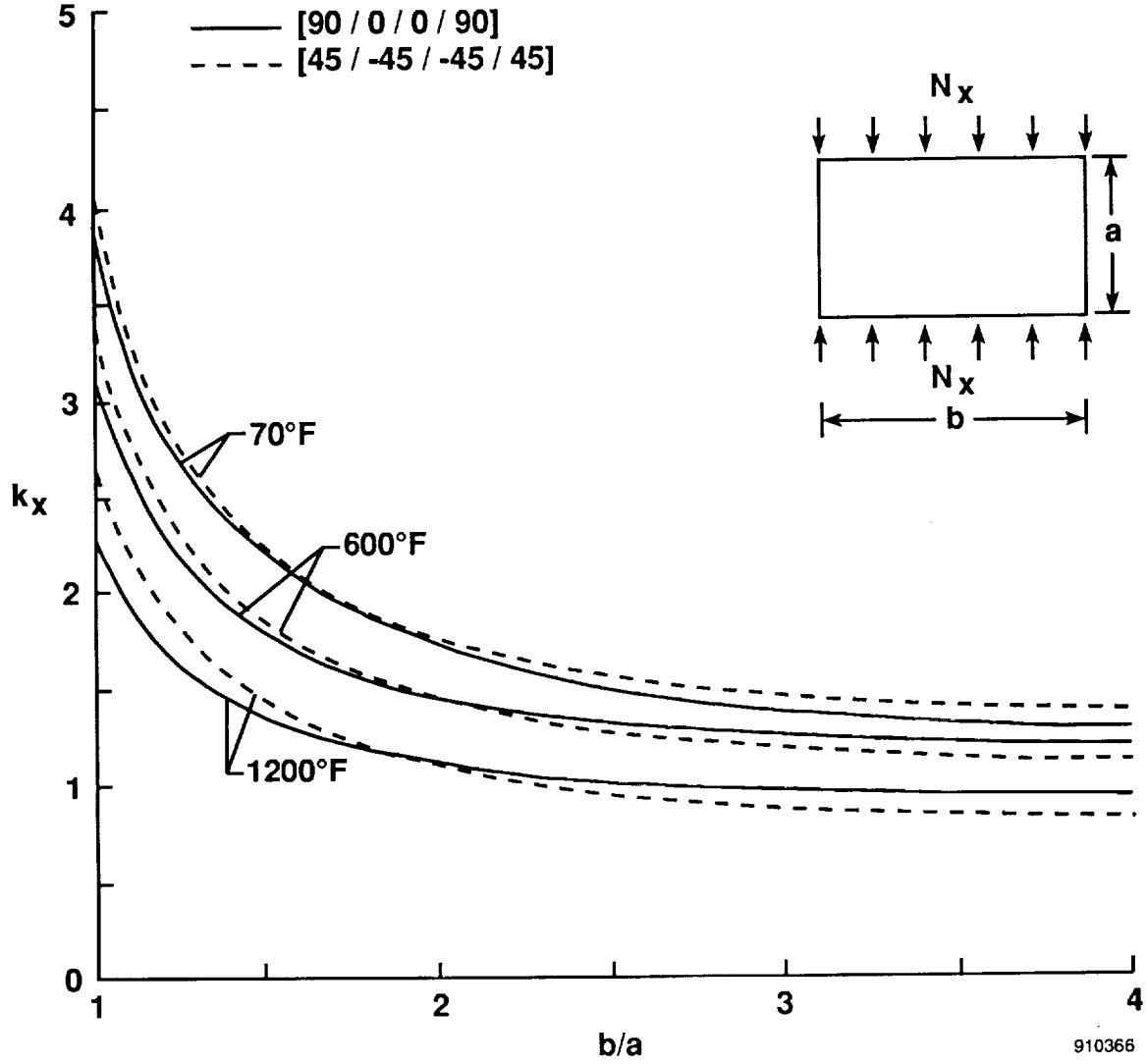

Figure 4. Degradation of compressive buckling strengths of metal matrix composite sandwich panels with increasing temperatures and aspect ratio; $SCS - 6/Ti - 15 - 3$ composite face sheets; $Ti - 6 - 4$ honeycomb core.

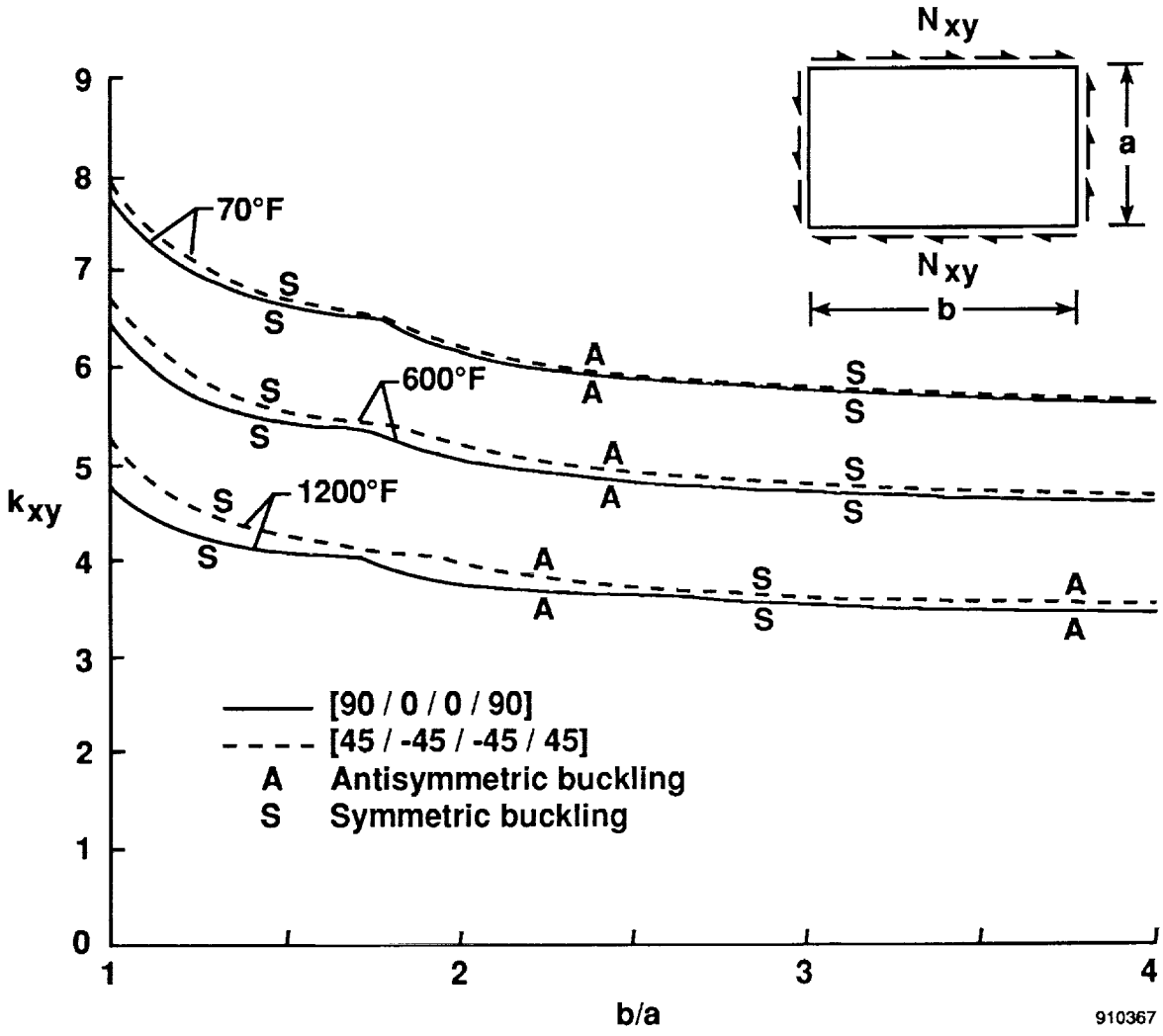

Figure 5. Degradation of shear buckling strengths of metal matrix composite sandwich panels with increasing temperatures and aspect ratio; $SCS-6/Ti-15-3$ composite face sheets; $Ti-6-4$ honeycomb core.

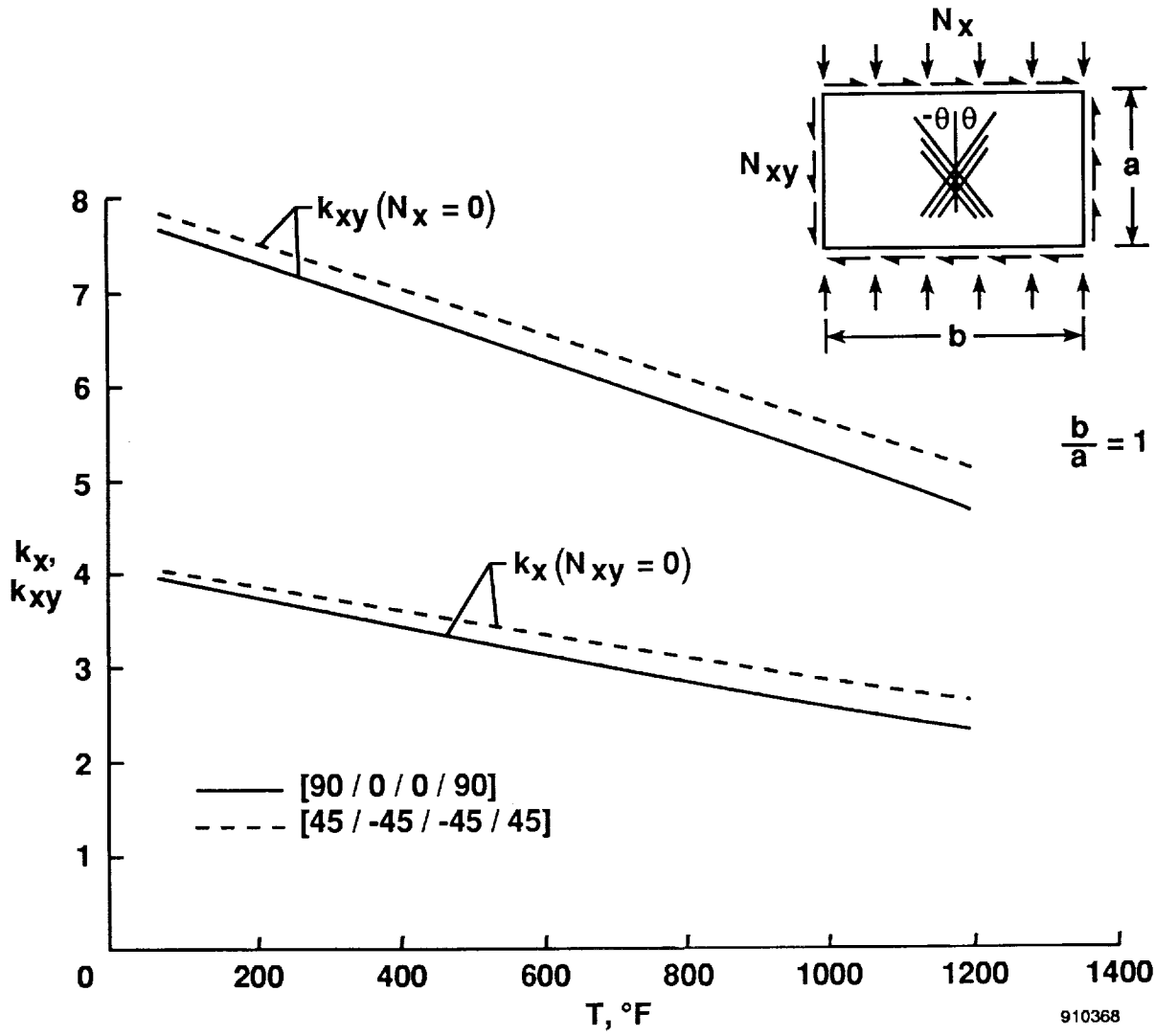

Figure 6. Degradation of buckling strengths of square metal matrix composite sandwich panels with temperatures; $SCS-6/Ti-15-3$ composite face sheets; $Ti-6-4$ honeycomb core.

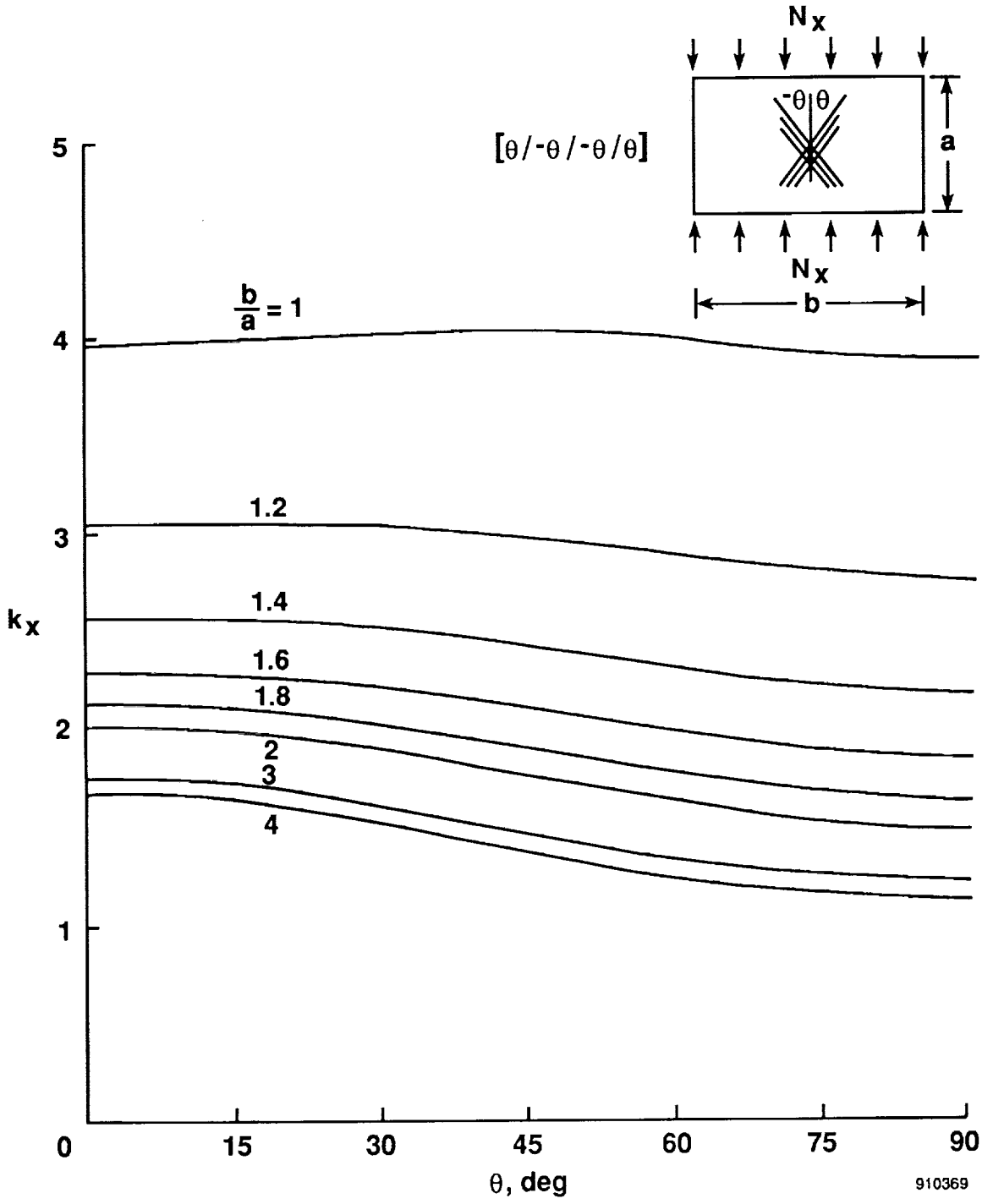

Figure 7. Effect of fiber orientation on compressive buckling strengths of metal matrix composite sandwich panels; $SCS - 6/Ti - 15 - 3$ composite face sheets; $Ti - 6 - 4$ honeycomb core; T = 70°F.

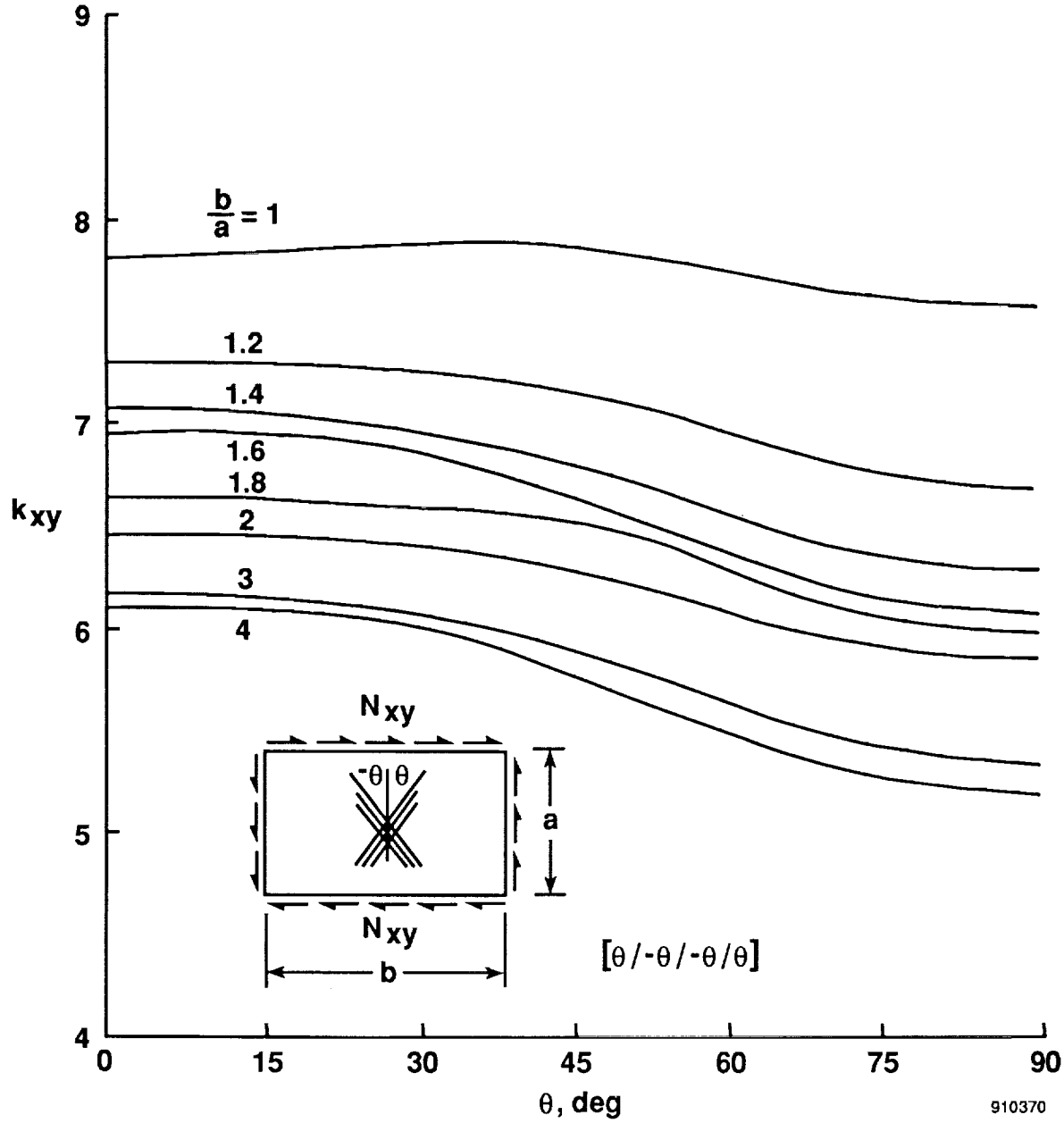

Figure 8. Effect of fiber orientation on shear buckling strengths of metal matrix composite sandwich panels; $SCS-6/Ti-15-3$ composite face sheets; $Ti-6-4$ honeycomb core.

REPORT DOCUMENTATION PAGE

Form Approved
OMB No. 0704-0188

1. AGENCY USE ONLY *(Leave blank)*	2. REPORT DATE	3. REPORT TYPE AND DATES COVERED
	September 1991	Technical Memorandum

4. TITLE AND SUBTITLE

Combined-Load Buckling Behavior of Metal-Matrix Composite Sandwich Panels Under Different Thermal Environments

5. FUNDING NUMBERS

RTOP 532-09-01

6. AUTHOR(S)

William L. Ko and Raymond H. Jackson

7. PERFORMING ORGANIZATION NAME(S) AND ADDRESS(ES)

NASA Dryden Flight Research Facility
P.O. Box 273
Edwards, California 93523-0273

8. PERFORMING ORGANIZATION REPORT NUMBER

H-1714

9. SPONSORING/MONITORING AGENCY NAME(S) AND ADDRESS(ES)

National Aeronautics and Space Administration
Washington, DC 20546-0001

10. SPONSORING/MONITORING AGENCY REPORT NUMBER

NASA TM-4321

11. SUPPLEMENTARY NOTES

12a. DISTRIBUTION/AVAILABILITY STATEMENT

Unclassified — Unlimited
Subject Category 39

12b. DISTRIBUTION CODE

13. ABSTRACT *(Maximum 200 words)*

Combined compressive and shear buckling analysis was conducted on flat rectangular sandwich panels with the consideration of transverse shear effects of the core. The sandwich panel is fabricated with titanium honeycomb core and laminated metal-matrix composite face sheets. The results show that the square panel has the highest combined-load buckling strength, and that the buckling strength decreases sharply with the increases of both temperature and panel aspect ratio. The effect of layup (fiber orientation) on the buckling strength of the panels was investigated in detail. The metal-matrix composite sandwich panel was much more efficient than the sandwich panel with nonreinforced face sheets and had the same specific weight.

14. SUBJECT TERMS

Combined load buckling; Honeycomb core; Metal matrix composites; Sandwich panels; Thermal environments

15. NUMBER OF PAGES

28

16. PRICE CODE

A03

17. SECURITY CLASSIFICATION OF REPORT	18. SECURITY CLASSIFICATION OF THIS PAGE	19. SECURITY CLASSIFICATION OF ABSTRACT	20. LIMITATION OF ABSTRACT
Unclassified	Unclassified	Unclassified	

NSN 7540-01-280-5500

Standard Form 298 (Rev. 2-89)
Prescribed by ANSI Std Z39-18
298-102

NASA-Langley, 1991